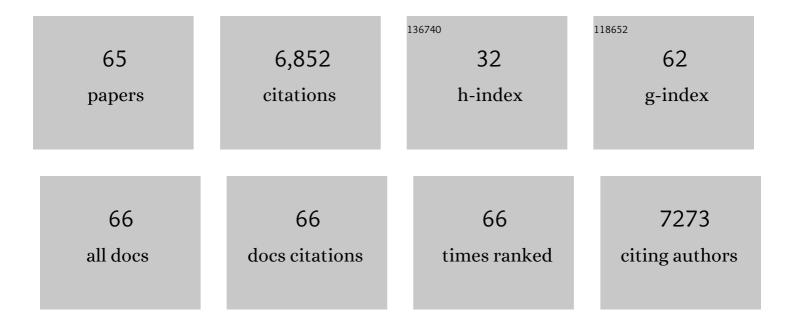
Andrea Zitolo

List of Publications by Year in descending order

Source: https://exaly.com/author-pdf/3442882/publications.pdf Version: 2024-02-01



ΔΝΙΏΡΕΛ ΖΙΤΟΙΟ

#	Article	IF	CITATIONS
1	Timeâ€Resolved Potentialâ€Induced Changes in Fe/N/Câ€Catalysts Studied by In Situ Modulation Excitation Xâ€Ray Absorption Spectroscopy. Advanced Energy Materials, 2022, 12, .	10.2	33
2	Au and Pt Remain Unoxidized on a CeO ₂ -Based Catalyst during the Water–Gas Shift Reaction. Journal of the American Chemical Society, 2022, 144, 446-453.	6.6	31
3	High loading of single atomic iron sites in Fe–NC oxygen reduction catalysts for proton exchange membrane fuel cells. Nature Catalysis, 2022, 5, 311-323.	16.1	248
4	Oxygen Reduction Reaction in Alkaline Media Causes Iron Leaching from Fe–N–C Electrocatalysts. Journal of the American Chemical Society, 2022, 144, 9753-9763.	6.6	59
5	Identification of durable and non-durable FeNx sites in Fe–N–C materials for proton exchange membrane fuel cells. Nature Catalysis, 2021, 4, 10-19.	16.1	368
6	Non-precious metal cathodes for anion exchange membrane fuel cells from ball-milled iron and nitrogen doped carbide-derived carbons. Renewable Energy, 2021, 167, 800-810.	4.3	50
7	Oxygen reduction reaction mechanism and kinetics on M-NxCy and M@N-C active sites present in model M-N-C catalysts under alkaline and acidic conditions. Journal of Solid State Electrochemistry, 2021, 25, 45-56.	1.2	59
8	The local atomic structure and thermoelectric properties of Ir-doped ZnO: hybrid DFT calculations and XAS experiments. Journal of Materials Chemistry C, 2021, 9, 4948-4960.	2.7	7
9	Stable Cr-MFI Catalysts for the Nonoxidative Dehydrogenation of Ethane: Catalytic Performance and Nature of the Active Sites. ACS Catalysis, 2021, 11, 3988-3995.	5.5	34
10	Potentialâ€Induced Spin Changes in Fe/N/C Electrocatalysts Assessed by In Situ Xâ€ray Emission Spectroscopy. Angewandte Chemie, 2021, 133, 11813-11818.	1.6	5
11	Potentialâ€Induced Spin Changes in Fe/N/C Electrocatalysts Assessed by In Situ Xâ€ray Emission Spectroscopy. Angewandte Chemie - International Edition, 2021, 60, 11707-11712.	7.2	36
12	The origin of the high electrochemical activity of pseudo-amorphous iridium oxides. Nature Communications, 2021, 12, 3935.	5.8	56
13	Metal Oxide Clusters on Nitrogen-Doped Carbon are Highly Selective for CO ₂ Electroreduction to CO. ACS Catalysis, 2021, 11, 10028-10042.	5.5	37
14	Enhancing the electrocatalytic activity of Fe phthalocyanines for the oxygen reduction reaction by the presence of axial ligands: Pyridine-functionalized single-walled carbon nanotubes. Electrochimica Acta, 2021, 398, 139263.	2.6	27
15	Understanding how single-atom site density drives the performance and durability of PGM-free Fe–N–C cathodes in anion exchange membrane fuel cells. Materials Today Advances, 2021, 12, 100179.	2.5	18
16	Carbonâ€Nanotubeâ€Supported Copper Polyphthalocyanine for Efficient and Selective Electrocatalytic CO ₂ Reduction to CO. ChemSusChem, 2020, 13, 173-179.	3.6	60
17	Evidence for an egg-box-like structure in iron(<scp>ii</scp>)–polygalacturonate hydrogels: a combined EXAFS and molecular dynamics simulation study. Physical Chemistry Chemical Physics, 2020, 22, 2963-2977.	1.3	14
18	Aerosol synthesis of thermally stable porous noble metals and alloys by using bi-functional templates. Materials Horizons, 2020, 7, 541-550.	6.4	13

ANDREA ZITOLO

#	Article	IF	CITATIONS
19	Evolution Pathway from Iron Compounds to Fe ₁ (II)–N ₄ Sites through Gas-Phase Iron during Pyrolysis. Journal of the American Chemical Society, 2020, 142, 1417-1423.	6.6	185
20	On the Influence of Oxygen on the Degradation of Feâ€N Catalysts. Angewandte Chemie, 2020, 132, 3261-3269.	1.6	133
21	On the Influence of Oxygen on the Degradation of Feâ€N Catalysts. Angewandte Chemie - International Edition, 2020, 59, 3235-3243.	7.2	160
22	P-block single-metal-site tin/nitrogen-doped carbon fuel cell cathode catalyst for oxygen reduction reaction. Nature Materials, 2020, 19, 1215-1223.	13.3	278
23	Revisiting the Sodiation Mechanism of TiO2 via Operando X-ray Absorption Spectroscopy. Applied Sciences (Switzerland), 2020, 10, 5547.	1.3	7
24	Water-Mediated ElectroHydrogenation of CO ₂ at Near-Equilibrium Potential by Carbon Nanotubes/Cerium Dioxide Nanohybrids. ACS Applied Energy Materials, 2020, 3, 8509-8518.	2.5	23
25	Activity–Selectivity Trends in the Electrochemical Production of Hydrogen Peroxide over Single-Site Metal–Nitrogen–Carbon Catalysts. Journal of the American Chemical Society, 2019, 141, 12372-12381.	6.6	493
26	Electroreduction of CO ₂ on Singleâ€6ite Copperâ€Nitrogenâ€Doped Carbon Material: Selective Formation of Ethanol and Reversible Restructuration of the Metal Sites. Angewandte Chemie, 2019, 131, 15242-15247.	1.6	43
27	Electroreduction of CO ₂ on Singleâ€Site Copperâ€Nitrogenâ€Doped Carbon Material: Selective Formation of Ethanol and Reversible Restructuration of the Metal Sites. Angewandte Chemie - International Edition, 2019, 58, 15098-15103.	7.2	369
28	Designing the 3D Architecture of PGM-Free Cathodes for H ₂ /Air Proton Exchange Membrane Fuel Cells. ACS Applied Energy Materials, 2019, 2, 7211-7222.	2.5	41
29	Volcano Trend in Electrocatalytic CO ₂ Reduction Activity over Atomically Dispersed Metal Sites on Nitrogen-Doped Carbon. ACS Catalysis, 2019, 9, 10426-10439.	5.5	142
30	Tuning the Structure of Galacturonate Hydrogels: External Gelation by Ca, Zn, or Fe Cationic Cross-Linkers. Biomacromolecules, 2019, 20, 2864-2872.	2.6	25
31	Effect of Pyrolysis Atmosphere and Electrolyte pH on the Oxygen Reduction Activity, Stability and Spectroscopic Signature of FeN _x Moieties in Fe-N-C Catalysts. Journal of the Electrochemical Society, 2019, 166, F3311-F3320.	1.3	70
32	The Challenge of Achieving a High Density of Fe-Based Active Sites in a Highly Graphitic Carbon Matrix. Catalysts, 2019, 9, 144.	1.6	22
33	Design of polygalacturonate hydrogels using iron(II) as cross-linkers: A promising route to protect bioavailable iron against oxidation. Carbohydrate Polymers, 2018, 188, 276-283.	5.1	27
34	Self-Assembly of the Nonplanar Fe(III) Phthalocyanine Small-Molecule: Unraveling the Impact on the Magnetic Properties of Organic Nanowires. Chemistry of Materials, 2018, 30, 879-887.	3.2	9
35	Short range order of As40-xCuxTe60 glasses. Journal of Non-Crystalline Solids, 2018, 481, 202-207.	1.5	1
36	Stabilization of Iron-Based Fuel Cell Catalysts by Non-Catalytic Platinum. Journal of the Electrochemical Society, 2018, 165, F1084-F1091.	1.3	33

ANDREA ZITOLO

#	Article	IF	CITATIONS
37	Physical and Chemical Considerations for Improving Catalytic Activity and Stability of Non-Precious-Metal Oxygen Reduction Reaction Catalysts. ACS Catalysis, 2018, 8, 11264-11276.	5.5	101
38	Electrochemical Reduction of CO ₂ Catalyzed by Fe-N-C Materials: A Structure–Selectivity Study. ACS Catalysis, 2017, 7, 1520-1525.	5.5	363
39	In Situ Observation of the Formation and Structure of Hydrogen-Evolving Amorphous Cobalt Electrocatalysts. ACS Energy Letters, 2017, 2, 2545-2551.	8.8	17
40	Identification of catalytic sites in cobalt-nitrogen-carbon materials for the oxygen reduction reaction. Nature Communications, 2017, 8, 957.	5.8	443
41	Changes in structure and conduction type upon addition of Ir to ZnO thin films. Thin Solid Films, 2017, 636, 694-701.	0.8	10
42	Synergy between molybdenum nitride and gold leading to platinum-like activity for hydrogen evolution. Physical Chemistry Chemical Physics, 2015, 17, 4047-4053.	1.3	38
43	Degradation by Hydrogen Peroxide of Metal-Nitrogen-Carbon Catalysts for Oxygen Reduction. Journal of the Electrochemical Society, 2015, 162, H403-H414.	1.3	161
44	Identification of catalytic sites for oxygen reduction in iron- and nitrogen-doped grapheneÂmaterials. Nature Materials, 2015, 14, 937-942.	13.3	1,714
45	Structural Characterization of Ionic Liquids by X-Ray Absorption Spectroscopy. Soft and Biological Matter, 2014, , 149-172.	0.3	0
46	On the possibility of using XANES to investigate bromide-based ionic liquids. Chemical Physics Letters, 2014, 591, 32-36.	1.2	12
47	K-edge XANES investigation of octakis(DMSO)lanthanoid(iii) complexes in DMSO solution and solid iodides. Physical Chemistry Chemical Physics, 2013, 15, 8684.	1.3	15
48	Using a Combined Theoretical and Experimental Approach to Understand the Structure and Dynamics of Imidazolium-Based Ionic Liquids/Water Mixtures. 2. EXAFS Spectroscopy. Journal of Physical Chemistry B, 2013, 117, 12516-12524.	1.2	50
49	Using a Combined Theoretical and Experimental Approach to Understand the Structure and Dynamics of Imidazolium-Based Ionic Liquids/Water Mixtures. 1. MD Simulations. Journal of Physical Chemistry B, 2013, 117, 12505-12515.	1.2	53
50	Hydration Properties of the Zn ²⁺ Ion in Water at High Pressure. Inorganic Chemistry, 2013, 52, 1141-1150.	1.9	41
51	X-ray Absorption Study of the Solvation Structure of Cu ²⁺ in Methanol and Dimethyl Sulfoxide. Inorganic Chemistry, 2012, 51, 8827-8833.	1.9	23
52	Effects of the Pathological Q212P Mutation on Human Prion Protein Non-Octarepeat Copper-Binding Site. Biochemistry, 2012, 51, 6068-6079.	1.2	32
53	Influence of the Second Coordination Shell on the XANES Spectra of the Zn ²⁺ Ion in Water and Methanol. ChemPlusChem, 2012, 77, 234-239.	1.3	40
54	Effect of the Zn ²⁺ and Hg ²⁺ lons on the Structure of Liquid Water. Journal of Physical Chemistry A, 2011, 115, 4798-4803.	1,1	34

ANDREA ZITOLO

#	Article	IF	CITATIONS
55	Revised Ionic Radii of Lanthanoid(III) Ions in Aqueous Solution. Inorganic Chemistry, 2011, 50, 4572-4579.	1.9	212
56	Structural characterization of zinc(II) chloride in aqueous solution and in the protic ionic liquid ethyl ammonium nitrate by x-ray absorption spectroscopy. Journal of Chemical Physics, 2011, 135, 154509.	1.2	33
57	X-Ray absorption spectroscopy investigation of 1-alkyl-3-methylimidazolium bromide salts. Journal of Chemical Physics, 2011, 135, 074505.	1.2	31
58	Analysis of the Detailed Configuration of Hydrated Lanthanoid(III) Ions in Aqueous Solution and Crystalline Salts by Using K―and L ₃ â€Edge XANES Spectroscopy. Chemistry - A European Journal, 2010, 16, 684-692.	1.7	73
59	X-ray absorption spectroscopy study of the solvation structure of zinc(II) in dimethyl sulfoxide solution. Chemical Physics Letters, 2010, 499, 113-116.	1.2	10
60	Cuprizone neurotoxicity, copper deficiency and neurodegeneration. NeuroToxicology, 2010, 31, 509-517.	1.4	59
61	Fe-heme structure in Cu,Zn superoxide dismutase from Haemophilus ducreyi by X-ray Absorption Spectroscopy. Archives of Biochemistry and Biophysics, 2010, 498, 43-49.	1.4	3
62	Structural Investigation of Lanthanoid Coordination: a Combined XANES and Molecular Dynamics Study. Inorganic Chemistry, 2009, 48, 10239-10248.	1.9	51
63	Ion hydration in high-density water. Journal of Physics: Conference Series, 2009, 190, 012057.	0.3	9
64	Measurement of x-ray multielectron photoexcitations at the <mml:math xmlns:mml="http://www.w3.org/1998/Math/MathML" display="inline"><mml:mrow><mml:msup><mml:mtext>I</mml:mtext><mml:mo>â^'</mml:mo></mml:msup>< Physical Review B, 2008, 78, .</mml:mrow></mml:math 	nml:mtex	t>
	Pure silica-supported transition metal catalysts for the non-ovidative dehydrogenation of ethane:		

⁵ confinement effects on the stability. Journal of Materials Chemistry A, 0, , .